TURBULENT FLOW CONTROL BY ELECTROMAGNETIC FORCES

Jean-François Dietiker*, Klaus A. Hoffmann**
*** Visiting Assistant Professor, ** Marvin J. Gordon Distinguished Professor**
Department of Aerospace Engineering
Wichita State University, Wichita, KS 67260, USA

Keywords: *Magnetohydrodynamics, Turbulence, Flow control*

Abstract

The possibility of controlling turbulent flow fields by the action of electromagnetic forces is numerically investigated. A suitable configuration of magnets and electrodes can generate a body force, called the Lorentz force that influences the boundary layer. Application of an appropriate electromagnetic field can decrease the skin friction coefficient over a turbulent supersonic flat plate. The vortex shedding generated behind a square cylinder can be altered.

1 Introduction

Magnetohydrodynamics (MHD) is the branch of fluid dynamics dealing with the interaction between an electromagnetic field and a velocity field. The fluid needs to be sufficiently electrically conducting for the electromagnetic field to have any significant effect [1]. A wide variety of MHD applications have been identified, ranging from high-speed aircraft propulsion systems [2], ship and submarine propulsion systems, radar systems, to power generators. When an electromagnetic field is applied to an electrically conducting fluid, an induced electric current is generated due to the fluid motion, and it produces a body force, known as the Lorentz force. This body force acts on the fluid, offering a new means of flow control. The Lorentz force tends to suppress turbulence by damping velocity fluctuations to a certain extent. Recent numerical investigations have shown that the MHD effect is beneficial for both laminar and turbulent flows. The possibility of delaying the boundary layer separation has been demonstrated both experimentally and numerically. The most appealing argument in utilizing MHD principles for aerospace engineering applications is the potential reduction in the skin friction coefficient and heat transfer. This can be obtained by applying a magnetic field perpendicular to the surface. This property was shown by Neuringer et al. [3] and McIlroy et al. [4] in 1958.

MHD phenomena are described by a system of partial differential equations. They are obtained by combining the Navier-Stokes equations (governing the motion of the fluid) and the Maxwell's equations (governing the electromagnetic field). The resulting set of equations is composed of eight equations (five for the Navier-Stokes equations and three for the magnetic induction equations). However, flows associated with aerospace engineering applications are generally characterized by a low electrical conductivity. Under this condition, the governing equations can be simplified. The resulting formulation is known as the low magnetic Reynolds number formulation. In this formulation, the magnetic field is considered as a given quantity and is not perturbed by the mean flow. The MHD effects are modeled by the introduction of source terms into the Navier-Stokes equations, representing the Lorentz force and Joule's heating.

Over the years, MHD research activities have been limited, and discontinued in time. In particular, there is a lack of experimental data, and most available experiments have been

conducted for liquid metal flows. It is possible to obtain some analytical solutions for simple cases, such as laminar flows over a flat plate under the influence of a magnetic field. Analytical solution for such flows is available from Rossow [5]. He obtained the equations representing an incompressible MHD boundary layer and subsequently derived expressions for the velocity profiles.

Inclusion of turbulence is essential to fully represent MHD flows. The first technique to model turbulence is called the Reynolds-Averaged approach. Turbulence is represented by a turbulent viscosity, which is added to the molecular viscosity. Turbulence models [6-8] are required to determine the turbulent viscosity from the mean flow quantities. The Reynolds-Averaged approach has been widely utilized due to its ease of implementation and numerical efficiency. However, numerical simulations of turbulent flows suffer from the inability of conventional turbulence models to deal with the large anisotropies of length scales associated with turbulence. Moreover, existing turbulence models are not designed for MHD flows and need to be modified and calibrated to account for the presence of electromagnetic fields. The lack of available experimental data renders this task challenging. The difficulty in developing a turbulence model for MHD flows lies in the fact that turbulence models are by nature non-universal.

The second approach for turbulent flow computation is the Large Eddy Simulation [9-10] (LES). Large scales are numerically computed, whereas the small scales are modeled by eddy viscosity models, known as Sub Grid Scale models (SGS). Algebraic models are sufficient, because the imperfections of these models should not greatly affect the solution. SGS models are assumed to be more homogeneous and less affected by the boundary conditions.

Several investigators have studied the influence of an electromagnetic field on the flow separation and the application of the Lorentz force to control a turbulent boundary layer. Crawford et al. [11] performed some numerical experimentations of turbulent channel flow of electrically conductive liquids subject to electromagnetic forces. Their configuration was such that the Lorentz force was acting in the streamwise direction, leading to an acceleration of the flow and an increase in drag. A typical arrangement of magnets and electrodes that generates a streamwise Lorentz force is illustrated in Fig. 1.

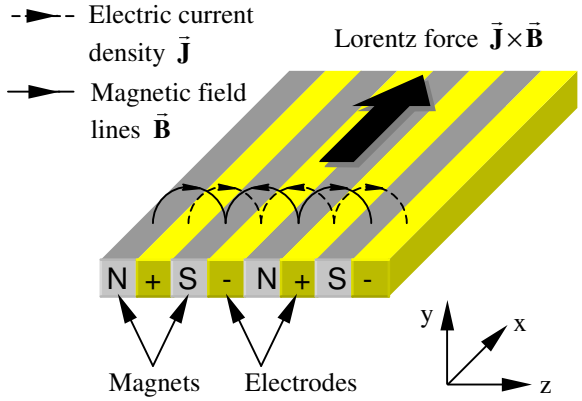

Figure 1. Magnets and electrodes arrangement generating a streamwise Lorentz force.

Other experimental studies on the influence of a streamwise Lorentz force on the flow over a flat plate in salt water were conducted by Weier et al. [12]. A strong acceleration of the fluid was achieved near the wall, delaying the stall of an inclined flat plate and a hydrofoil. All of these investigations were conducted for low Reynolds number and low magnetic Reynolds number flows, when the electrical conductivity of the fluid is small. However, low magnetic Reynolds number flows can also be encountered for high speed flows, even in supersonic regime. Gaitonde et al. [13] studied a supersonic flat plate boundary layer flow in presence of a non-uniform magnetic field and no electric field, which leads to a deceleration of the flow in the boundary layer and a decrease in the skin friction coefficient.

Most of the research combining the effect of turbulence with magnetohydrodynamics has been conducted for flows of liquid metals in simple geometries or in astrophysical applications, where the length scales are very large. Basic observations tend to show that the presence of a magnetic field would inhibit turbulence [14-15]. The interaction between

magnetic, electric and flow fields can be used to generate a Lorentz force that would decrease the level of velocity fluctuations, which is one of the characteristics of turbulent flows. The presence of the magnetic field provides another form of energy and new means of energy transfer within the flow field [16-17]. When the effect of the magnetic field has been incorporated in the turbulence models, it has usually resulted in the addition of a negative turbulent viscosity [18-19]. A process of relaminarization has also been identified to be a feature of turbulent MHD flows [20].

MHD flow control provides a prospective method that could be used in many industrial applications, ranging from power generation, propulsion systems to hypersonic vehicles and atmospheric reentry vehicles. The objective of this study is to investigate the possibility of controlling a boundary layer by means of electromagnetic forces. Some assumptions are imposed to simplify the implementation of the numerical schemes. The fluid is assumed to have a low electrical conductivity, such that the low magnetic Reynolds number formulation can be employed. The Reynolds-Averaged approach is used for compressible flows due to its ease of implementation and numerical efficiency. However, existing turbulence models are not designed for MHD flows and need to be modified and calibrated to account for the presence of electromagnetic fields. Such modifications are included in the current investigation. Several turbulence models are compared and the effect of the magnetic field on the skin friction coefficient is investigated. Large Eddy Simulation with Smagorinsky Sub Grid Scale model is employed for incompressible flow fields. The commercial finite volume CFD code FLUENT is used as the incompressible Navier-Stokes solver. The MHD source terms are added through user-defined functions. The computation of a flow field over a square cylinder is considered. When no magnetic field is present, a pair of shedding vortices is generated and convected in the wake of the cylinder. The possibility of reducing the vortex shedding by adding an electromagnetic field is being addressed.

2 Governing Equations

The numerical simulation of MHD flows typically requires the solution of a system of eight equations: continuity, momentum (three components), energy, and magnetic field induction (three components). For magneto-hydrodynamic flows that are characterized by a low electrical conductivity, the governing equations can be simplified. The validity of the simplification is monitored by a non-dimensional number known as the magnetic Reynolds number, which represents the ratio of the magnetic convection to the magnetic diffusion. It is defined as $Re_m = \sigma_e \mu_e U_\infty L$, where σ_e is the electrical conductivity of the fluid, μ_e is the electrical permeability, U_∞ and L are respectively the reference velocity and reference length. It can be shown that for small values of the magnetic Reynolds number ($Re_{m\infty} << 1$), the induced magnetic field is negligible compared to the applied magnetic field. Therefore, when this assumption is valid, the magnetic induction equations do not need to be solved. This is especially appealing since the resolution of these equations is the source of numerical difficulties. When the full system of MHD equations is solved, it has been experienced to be very difficult for the magnetic field to remain divergence-free at all time levels. Numerical techniques have been proposed [21] to alleviate this problem, but generally result in more complex equations or additional steps in the numerical procedure. The other source of difficulty is that the MHD equations become stiffer as the magnetic Reynolds number decreases. In the low magnetic Reynolds number approach, the magnetic field automatically satisfies the zero-divergence constrain, provided its initial distribution is divergence free (since it is given and remains constant through the computation). The current density is determined directly from the Ohm's law and the MHD effect is modeled by the introduction of source terms in the Navier-Stokes equations. Under the assumption of small magnetic Reynolds number, the governing equations are:

Continuity equation:

$$\frac{\partial \rho}{\partial t} + \vec{\nabla} \cdot \left(\rho \vec{U} \right) = 0 \qquad (1)$$

Momentum equation:

$$\frac{\partial \left(\rho \vec{U} \right)}{\partial t} + \vec{\nabla} \cdot \left[\rho \vec{U} \otimes \vec{U} + p \overline{\overline{I}} \right] = \vec{\nabla} \cdot \overline{\overline{\tau}} + \vec{J} \times \vec{B} \qquad (2)$$

and, Energy equation:

$$\frac{\partial}{\partial t}(\rho e_t) + \vec{\nabla} \cdot \left[(\rho e_t + p) \vec{U} \right] = \vec{\nabla} \cdot \left(\vec{U} \cdot \overline{\overline{\tau}} \right) \backslash - \vec{\nabla} \cdot \vec{Q} + \vec{E} \cdot \vec{J} \qquad (3)$$

The current density can be evaluated from the Ohm's law

$$\vec{J} = \sigma_e \left(\vec{E} + \vec{U} \times \vec{B} \right) \qquad (4)$$

The equations are solved by a modified fourth-order Runge-Kutta scheme augmented with a second order TVD scheme. Details of the numerical scheme can be found in Ref. 22. This explicit scheme has been demonstrated to be very robust, especially for problems involving shock waves [23-27]. RAMHD2D is the finite difference compressible code developed for this study. It provides several turbulence models based on the Reynolds-averaged equations of motion, ranging from algebraic model (Baldwin-Lomax), one-equation turbulence models (Baldwin-Barth and Spalart-Allmaras) and two-equation models (k-ϵ and k-ϵ / k-ω models).

The finite volume computer code *FLUENT* is used to solve the incompressible equations. A complete description of the available numerical schemes can be obtained from *FLUENT* user guide [28]. Mass conservation is enforced by using a relation between velocity and pressure correction (SIMPLE algorithm). Momentum equations are approximated by second-order central-differencing discretization scheme. For the LES, the standard Smagorinsky Sub-Grid-Scale model has been used with a value of $C_s = 0.1$ for the Smagorinsky constant.

3 Results

3.1 Flow over a Flat Plate

The objective of this section is to investigate the effect of the magnetic field on the skin friction coefficient for a supersonic turbulent flow over a flat plate. The freestream conditions are summarized in Table 1. The length of the flat plate is $0.08\,\text{m}$ and the transition is triggered at $x = 0.04\,\text{m}$. The magnetic Reynolds number based on the length of the flat plate is $\text{Re}_m = 0.058$, which can be considered negligible compared to one. A schematic of a typical flow is illustrated in Fig. 2.

Property	Symbol	Value
Mach number	M_∞	2.0
Pressure	p_∞	1.0 atm
Temperature	T_∞	300.0 K
Reynolds number	Re_∞	3.75×10^6
Electrical conductivity	$\sigma_{e\infty}$	800 mho / m

Table 1. Flow properties over the flat plate.

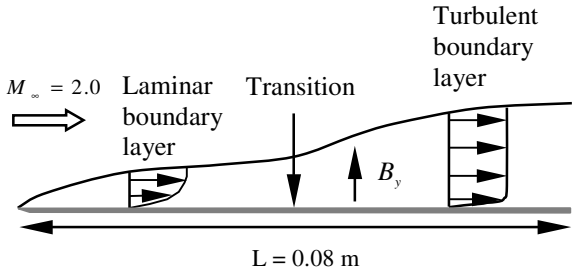

Figure 2. Schematic of the flow over a flat plate.

The grid system consists of 100 grid points in the $x-$direction and 50 in the $y-$direction. Grid point clustering has been implemented near the leading edge to capture the weak leading edge shock wave and near the solid surface to resolve the boundary layer. The plate is considered to be an adiabatic wall.

The magnetic field is applied in the $y-$direction, ranging from zero to $1.4\,\text{T}$. The strength of the magnetic field can be represented either by the magnitude of the applied magnetic

field B_y, or by the parameter m (interaction parameter per unit length). The relation between B_y and m is provided in Equation (5).

$$m = \frac{\sigma_{e\infty} B_y^2}{\rho_\infty U_\infty} \qquad (5)$$

First, all the turbulence models are compared in the non-magnetic case. Figure 3 illustrates the skin friction coefficient along the flat plate. Transition from laminar to turbulent flow is triggered at $x = 0.04$ m. In the turbulent region, all turbulence models provide a skin friction coefficient that falls between the analytical solution and the pseudo empirical method of Spalding and Chi [29].

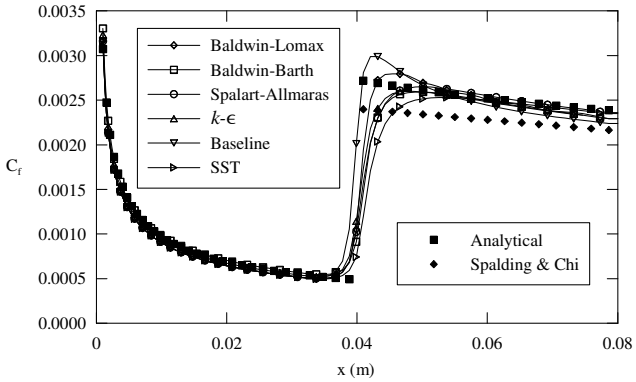

Figure 3. Comparison of all turbulence models.

Next, the magnetic field is turned on in the $y-$direction. Figure 4 shows the skin friction coefficient obtained by the Baldwin-Lomax model for different values of the magnetic field. The skin friction coefficient is decreased in the laminar region as the magnetic field is increased. The same effect can be observed in the turbulent region.

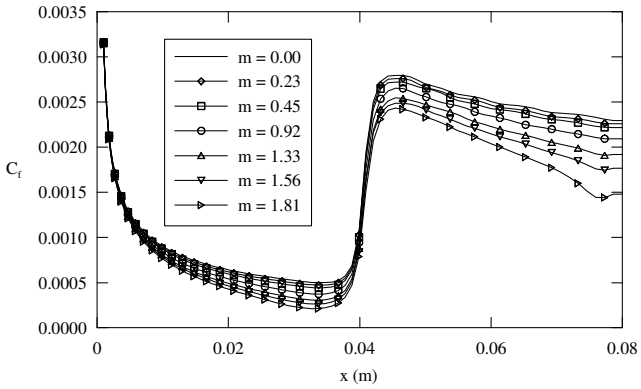

Figure 4. Skin friction coefficients (Baldwin-Lomax model).

Figure 5 illustrates the turbulent velocity profile obtained by the Baldwin-Lomax turbulence model, at $x = 0.06$ m. In the turbulent case, it is possible to increase the magnetic field up to $m = 1.81$, after which a massive separation occurs. The separation occurs for a higher magnetic field compared to the laminar case because the turbulent layer can sustain stronger Lorentz force. This is similar to the comparison between laminar and turbulent boundary layers subject to adverse pressure gradient. The separation is delayed when the boundary layer is turbulent.

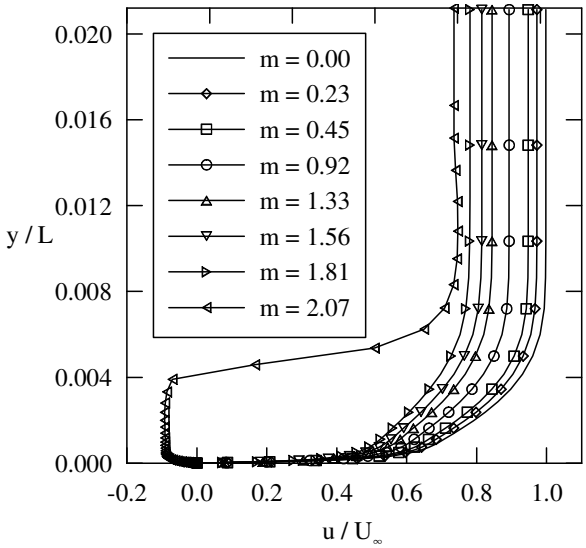

Figure 5. Turbulent velocity profiles at $x = 0.06$ m (Baldwin-Lomax model).

Similar results are obtained with the other turbulence models. For all turbulence models, a separation consistently occurred when m was greater than 1.81. Figure 6 illustrates the turbulent velocity profiles obtained by all turbulence models in the non-magnetic case. A good consistency between the turbulence models can be observed. For a magnetic field corresponding to $m = 1.33$ (Fig. 7), all turbulence models provide similar velocity profiles. It should be noted that the freestream velocity is reduced by about 12% when the magnetic field is turned on.

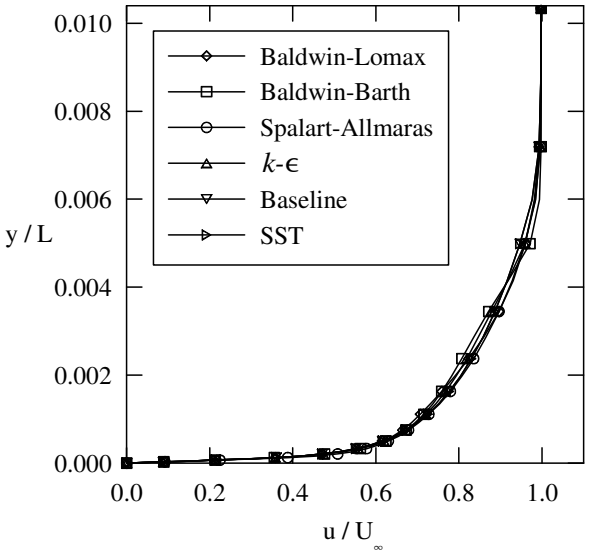

Figure 6. Comparison of turbulent velocity profiles at $m = 0.00$.

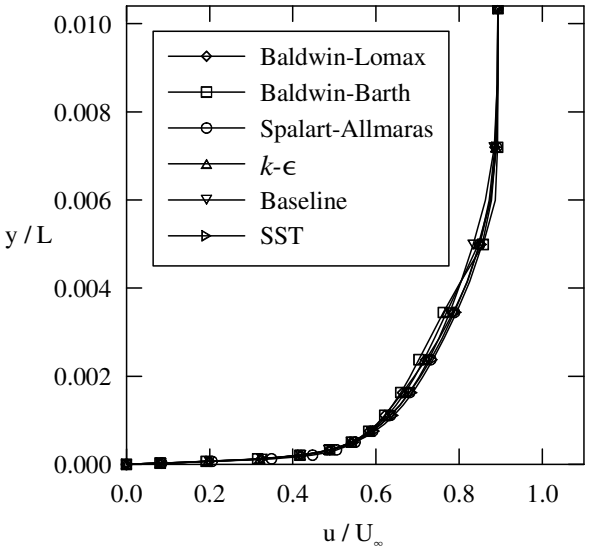

Figure 7. Comparison of turbulent velocity profiles at $m = 1.33$.

Figure 8 presents a comparison of all turbulence models at $m = 1.33$. The models are consistent with each other, except in the region immediately beyond the transition point. Figure 9 shows the skin friction coefficients at a given location ($x = 0.06\,m$), when it is normalized with its non-magnetic counterpart. In the laminar case, the reduction of the skin friction coefficient is larger than in the turbulent case. A substantial reduction is achieved, which leads to the separation of the flow (negative value of the skin friction coefficient). In the turbulent case, a reduction of up to about 20% is achieved with all turbulence models, at the highest value of magnetic field. For high conductivity fluids, a relaminarization process was observed [30], where the turbulent skin friction coefficient could be substantially reduced, reaching the same value as the laminar skin friction coefficient. Here, a complete relaminarization of the flow cannot be achieved because the effect of the magnetic field on the mean flow is more significant than the effect on the small scales of motion. A flow separation occurs before the relaminarization of the flow is achieved.

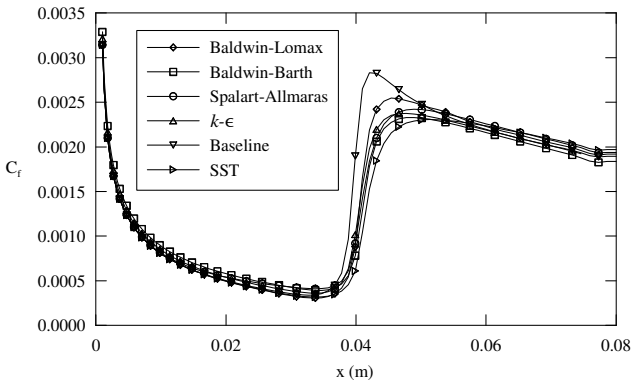

Figure 8. Comparison of all turbulence models at $m = 1.33$.

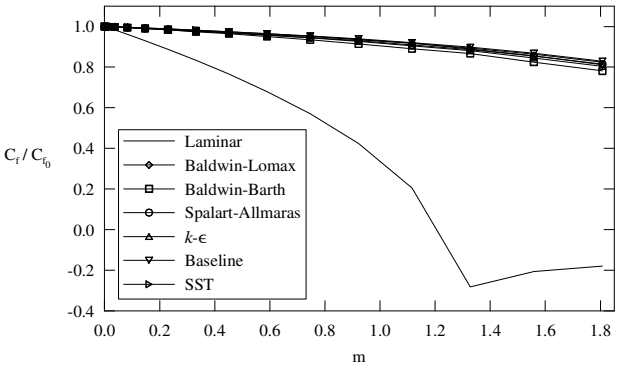

Figure 9. Skin friction coefficient ratio obtained by all turbulence models.

3.2 Flow over a square cylinder

The turbulent flow over a square cylinder is investigated in this section. The geometry of the problem is illustrated in Fig. 10. The diameter of the cylinder is $D = 0.04\,m$. The incoming velocity is $U = 0.535\,m/sec$. The fluid is salt water. The Reynolds number based on the

incoming velocity and cylinder diameter is $\mathrm{Re} = 21{,}400$. Experimental data is available based on experiments by Lyn and Rodi [31]. A summary of experimental results is provided in Table 2.

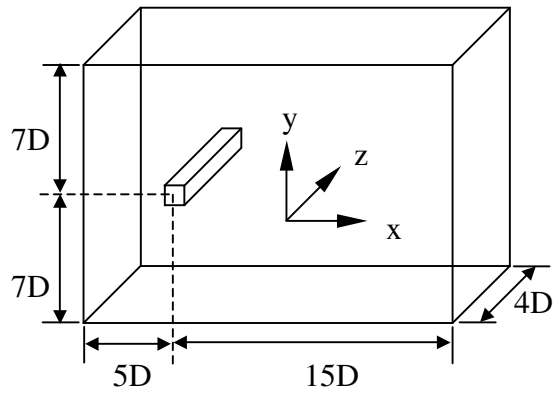

Figure 10. Geometry for the turbulent flow over a square cylinder.

Quantity	Experimental data	Numerical value
Strouhal Number	0.130	0.131
Mean reattachment length	1.38D	1.20D
Mean drag coefficient	0.19 to 0.21	0.18
Lift coefficient rms	0.6 to 1.4	0.9

Table 2. Summary of experimental and numerical results for the turbulent flow over a square cylinder.

Initially, the computation was carried out without the application of any magnetic field. This condition corresponds to the experimental set up. A first grid, consisting of 204,000 nodes and 368,000 wedge cells did not provide satisfactory results and was refined several times. The finest grid consisted of 968,000 nodes and 1.8 million wedge cells. Second order central differencing was used with the standard Smagorinsky model with $C_s = 0.1$. A free stream turbulence intensity of 2% was imposed at the inflow. Symmetry is imposed along the lateral boundaries. The mesh was stretched at the cylinder surface with a minimum wall spacing of about $D/140$ in the normal direction.

The computation was carried out for at least 40 shedding cycles to obtain sensible averages. The time step was reduced until the Strouhal number matched the experimental data. For the smallest time step $\Delta t = 0.002\,\mathrm{sec}$, the numerical simulation provided a Strouhal number of 0.131, which is in good agreement with the experimental value $\mathrm{St} = 0.13$. Other average quantities are summarized in Table 2. Fairly good agreement is achieved between the numerical and experimental data. Figure 11 illustrates an iso-surface of the vorticity, colored by static pressure (x-y plane).

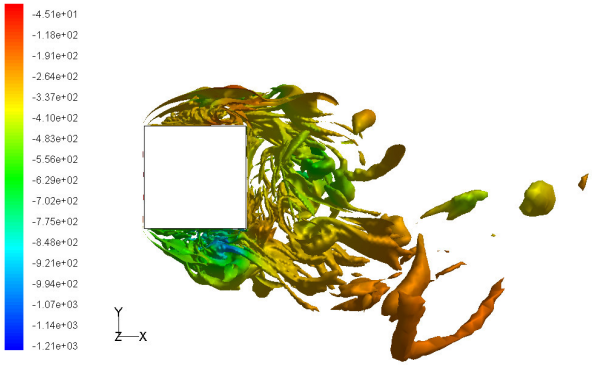

Figure 11. Isosurface of vorticity, colored by static pressure (x-y plane).

Next, the effect of the magnetic field is investigated. The magnetic field is applied perpendicularly to the cylinder walls. The magnitude of the magnetic field decreases exponentially away from the walls of the cylinder. Since the magnetic field is essentially zero a few diameters away from the cylinder, it does not influence the boundary conditions. The electrical conductivity of the salt water is $\sigma_e = 100\,\mathrm{mho/m}$. The corresponding magnetic Reynolds number is 2.7×10^{-6}, and the low magnetic Reynolds number formulation is valid to describe the flow.

The application of a magnetic field has a direct influence on the flow pattern as depicted in Fig. 12. As the strength of the magnetic field increases, the shedding vortices move towards the cylinder. The corresponding reattachment length decreases and is illustrated in Fig. 13a. This corresponds to an increase in the average drag (Fig. 13b). However, the frequency of the

shedding vortices starts to increase for moderate magnetic field (Fig. 13c), and subsequently decreases for a large value of the magnetic field ($B_0 = 15\,T$). The lift coefficient fluctuation substantially increases for large magnetic fields (Fig. 13d). In all cases, the average lift coefficient remained zero.

No electric field was imposed in any of these calculations. Therefore, the Lorentz force always acts in the opposite direction of the velocity, and tends to slow down the flow. This usually results in a decrease in the skin friction coefficient along the wall. However, for a complex flow with large separation regions, the skin friction drag represents only a fraction of the total drag. Therefore, the benefit obtained from the application of a magnetic field is not sufficient to reduce the total drag. Moreover, the standard Smagorinsky model was implemented, with the assumption that the magnetic field does not affect the Sub-Grid-Scale model. Modification to account for the presence of a magnetic field could result in different conclusions. The introduction of damping terms into the SGS models, and modification of the Smagorinsky constant are currently under consideration.

4 Conclusions

The possibility of controlling the boundary layer by means of electromagnetic forces has been numerically investigated. The low electrical conductivity of the fluid results in a simplification of the equations, where the MHD contribution is modeled by additional source terms in the Navier-Stokes equations. A reduction of up to 20% in the turbulent skin friction coefficient can be achieved by applying a magnetic field over a supersonic flat plate, before a separation of the flow field occurs. For the flow over a square cylinder, the application of a magnetic field resulted in an increase in the drag and decrease in the reattachment length.

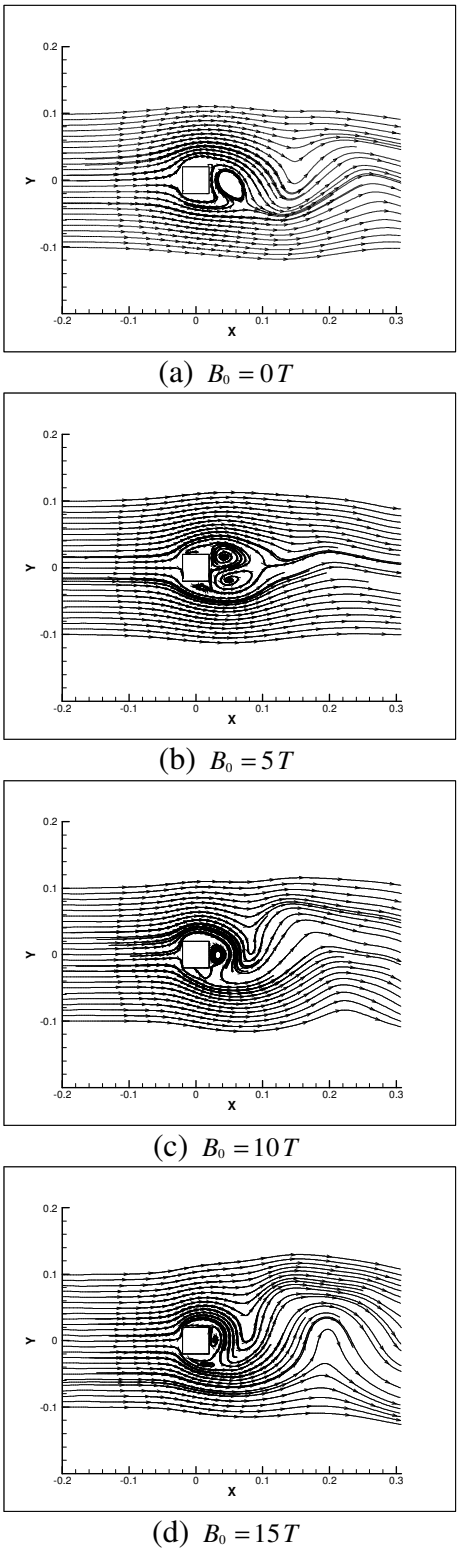

Figure 12. Streamline pattern for several values of the applied magnetic field.

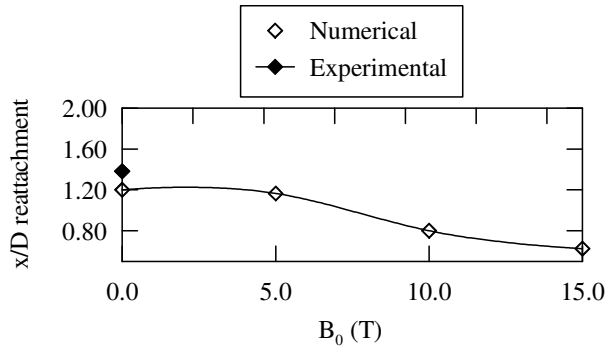

(a) Mean reattachment length.

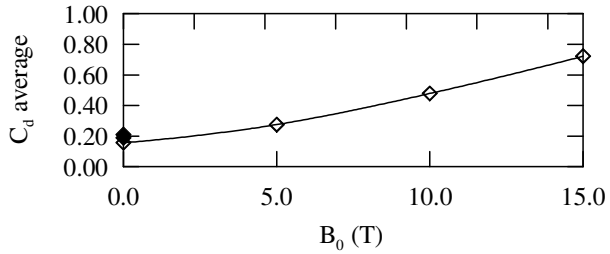

(b) Mean drag coefficient.

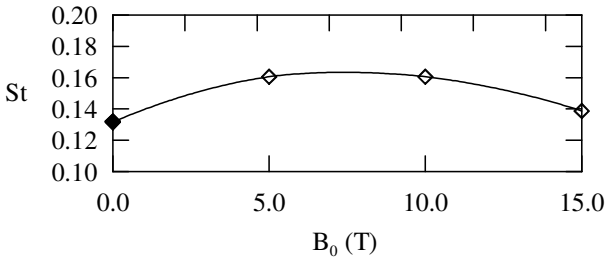

(c) Strouhal number.

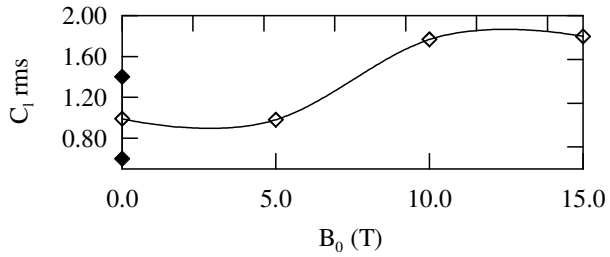

(d) Lift coefficient rms fluctuations.

Figure 13. Effects of the applied magnetic field.

References

[1] Rosa R. *Magnetohydrodynamic energy conversion.* McGraw-Hill Book Company, 1968.

[2] Stuhlinger E. *Ion Propulsion for Space Flight.* McGraw-Hill Book Company, 1964.

[3] Neuringer J, and McIlroy W. Incompressible two-dimensional stagnation point flow of an electrically conducting viscous fluid in the presence of a magnetic field. *Journal of the Aeronautical Sciences*, Vol. 25, No.3, pp. 194-198, March 1958.

[4] McIlroy W, and Neuringer J. Hydromagnetic effects on stagnation point heat transfer. *Journal of the aeronautical sciences*, Vol. 25, No. 5, pp. 332-335, May 1958.

[5] Rossow J. On flow of electrically conducting fluids over a flat plate in the presence of a transverse magnetic field. NACA TN 3971, May 1957.

[6] Baldwin B, and Lomax H. Thin layer approximation and algebraic model for separated turbulent flows. AIAA paper 78-257, January 1978.

[7] Baldwin B, and Barth T. A one-equation turbulent transport model for high Reynolds number wall-bounded flows. NASA TM 102847, August 1990.

[8] Spalart P, and Allmaras S. A one-equation turbulence model for aerodynamic flows. AIAA paper 92-0439, January 1992.

[9] Lesieur M, and Comte P. Large eddy simulations of compressible turbulent flows. Turbulence in Compressible Flows, AGARD report No. 819, 1997.

[10] Sagaut P. *Introduction à la simulation des grandes echelles pour les ecoulements de fluide incompressible.* Springer-Verlag Berlin, 1998.

[11] Crawford C, and Karniadakis G. Reynolds stress analysis of EMHD-controlled wall turbulence. Part I. Streamwise forcing. *Physics of fluids*, Vol. 9, No. 3, March 1997.

[12] Weier T, Fey U, Gerbeth G, Mutschke G, and Avilov V, Boundary layer control by means of electromagnetic forces. ERCOFTAC bulletin 44, pp. 36-40, 2000.

[13] Gaitonde D, and Poggie J. Simulation of MHD flow control techniques. AIAA paper 2000-2326, Fluid 2000, June 2000.

[14] Ferraro, and Plumton, *Magneto-Fluid Mechanics*, Oxford University press, 1966.

[15] Napolitano L. On turbulent magneto-fluid dynamic boundary layers. *Review of modern physics*, Vol. 32, pp. 785-795, October 1960.

[16] Lykoudis P. Transition from laminar to turbulent flow in magneto-fluid mechanic channels. *Review of modern physics*, Vol. 32, pp. 796-798, October 1960.

[17] Chandrasekhar. Hydromagnetic turbulence, II An elementary theory. *Proc. Roy. Soc*. A233, 330, 1955.

[18] Shimomura. Large eddy simulation of magnetohydrodynamics turbulent channel flows under a uniform magnetic field. *Physics of fluids,* A3 (12) pp. 3098-3106, December 1991.

[19] Sukoriansky. Stabilized negative viscosity as sub grid scale representation of two dimensional turbulence. Progress in fluid flow research: turbulence and applied MHD (*Progress in astronautics and aeronautics*, Vol. 182), pp. 33-47, 1998.

[20] Narasimha. Relaminarization - MHD and otherwise. Liquid-metal flows and magnetohydrodynamics: the third international seminar in the MHD flows and turbulence series (*Progress in astronautics and aeronautics*, Vol. 84), pp. 30-52, 1983.

[21] Powell K, Roe P, Myong R, Gombosi T, and De Zeeuw D. An upwind scheme for magneto-hydrodynamics. AIAA paper 95-1704-C, June 1995.

[22] Hoffmann K, Damevin H-M, and Dietiker J-F. Numerical simulation of hypersonic magnetohydrodynamic flows. *AIAA 31st Plasmadynamics and Lasers Conference*, AIAA-2000-2259, June 2000.

[23] Harada S, Augustinus J, Hoffmann K, and Agarwal R. Development of a modified Runge-Kutta scheme with TVD limiters for the ideal 1-D MHD equations. *13th AIAA Computational Fluid Dynamics Conference*, AIAA-97-2090, June 1997.

[24] Augustinus J, Harada S, Hoffmann K, and Agarwal R. Numerical solution of the eight-wave structure ideal MHD equations by modified Runge-Kutta scheme with TVD. AIAA 28th Plasmadynamics and Lasers Conference, AIAA-97-2398, June 1997.

[25] Augustinus J, Hoffmann K, and Harada S. Effect of magnetic field on the structure of high–speed flows. *Journal of Spacecraft and Rockets*, Vol. 35, No. 5, pp. 639-646, September-October 1998.

[26] Harada S, Hoffmann K, and Augustinus J. Numerical solution of the ideal magnetohydrodynamics equations for a supersonic channel flow. *Journal of thermophysics and heat transfer*, Vol. 12, No. 4, pp. 507-513, October-December 1998.

[27] Harada S, Hoffmann K, and Augustinus J. Development of a modified Runge-Kutta scheme with TVD limiters for the ideal two-dimensional MHD equations. AIAA-98-0981, January 1998.

[28] http://www.fluent.com.

[29] Spalding D, Chi S. The drag of a compressible turbulent boundary layer on a smooth plate with and without heat transfer. *Journal of fluid mechanics*, Vol. 18, No. 1, pp. 117-143, 1964.

[30] Dietiker J-F, and Hoffmann K. Numerical simulation of turbulent magnetohydrodynamic flows. *32nd AIAA Plasmadynamics and laser Conference*, AIAA paper 2001-2737, June 2001.

[31] Lyn D, and Rodi W. The flapping shear layer formed by flow separation from the forward corner of a square cylinder. *Journal of fluid mechanics*, Vol. 267, pp. 353-376, 1994.